SPECIFIC USE OF NON-METALLIC INCLUSIONS FOR THE FORMATION OF ACICULAR FERRITE STRUCTURES: THERMODYNAMIC MODELING AND LABORATORY EXPERIMENTS

D. Loder and S.K. Michelic
(Chair of Ferrous Metallurgy, Montanuniversitaet Leoben, Austria)

ABSTRACT
Non-metallic inclusions have a significant impact on steel properties. Whereas most applications require a high level of cleanness, meaning a possibly low content of inclusions, the present study deals with the specific use of non-metallic inclusions for the adjustment of a defined microstructure. Acicular ferrite nucleates intergranularly at non-metallic inclusions and provides excellent toughness; thus, by increasing the amount of acicular ferrite in the microstructure steel properties can be improved significantly. Nevertheless, in order to obtain the desired microstructure, a very precise control of the cleanness level is necessary. Not only the inclusion number, but especially their composition and size determine their potential for acicular ferrite nucleation. The present study focuses on the adjustment of defined cleanness conditions in HSLA steels favourable for the subsequent formation of acicular ferrite. Two different steel types are investigated, which only differ in the used deoxidizer. For this purpose thermodynamic calculations and experiments on laboratory scale in a so called Tammann Furnace are applied. Manual and automated SEM/EDS analyses are used for inclusion characterization in the steel samples. Finally, the samples produced in the Tammann Furnace are investigated by High Temperature Laser Scanning Confocal Microscopy (HT-LSCM). This method enables the in-situ observation of the acicular ferrite nucleation on non-metallic inclusions. So, the impact of different inclusion types on the acicular ferrite formation is demonstrated.

INTRODUCTION
Principally, non-metallic inclusions (NMI) are known to negatively affect steel properties. Thus, considerable research work was done aiming in the reduction of NMI in the matrix in order to improve the mechanical characteristics of steels. But in the past few years a contrary approach emerged: Appropriate tailored NMI are used to modify the microstructure and improve steel properties significantly [1–3]. Especially the formation of acicular ferrite, which uses NMI inside the austenite grain as nuclei, turned out to achieve a substantial increase in toughness due to the significant differences in the propagation path for cleavage cracks compared to other microstructures [4]. In a first step, knowledge about the influence of NMI on the formation of acicular ferrite was gained by studies on weldments in the fusion zone [5–9]. Based on these first approaches, significant effort has been spent on finding an appropriate method for the creation of acicular ferrite by means of thermomechanical treatments. The latter was mainly focused on so-called HSLA (High Strength Low Alloyed) steels [10]. At present, it is well known that the nucleation of acicular ferrite is mainly affected by steel composition, cooling rate, austenite grain size as well as the size, number and chemical composition of NMI [10, 11]. Sarma et al. [10] gave a comprehensive review on the influence of inclusion composition on the formation of acicular ferrite, in which particularly Ti- and Mn-containing complex inclusions are described as active nuclei for acicular ferrite. In order to achieve these kinds of particles in the steel, most previously published studies add oxide powders or very small particles to the steel melt. Thus, the inclusions are not formed due to reactions or interactions in the liquid melt, but are added artificially [12–14]. The present study deals with the specific use of deoxidation and desulfurization products, which are formed directly during steel making. For that reason the knowledge about inclusion formation and modification during processing is essential. So, although the aim of the current project is

contrary to conventional researches concerning steel cleanness, the requirements are quite the same: In order to control the inclusion landscape, an accurate prediction and the systematic handling of influencing factors is very important. Thermodynamic software, like *FactSage*, provides the possibility to model the formation of NMI during processing as well as inclusion modification during solidification [15, 16]. The focus of the present work is the evaluation of endogenous inclusion types regarding their tendency for acicular ferrite formation in two HSLA steels, which only differ in the used deoxidizers. For that purpose thermodynamic calculations and laboratory experiments in a Tammann type furnace are linked. Thermodynamic calculations are used to design the laboratory experiments and to predict the final inclusion landscape. In a second step, the produced steel samples are heat treated using a high-temperature laser scanning confocal microscopy (HT-LSCM), which enables the in situ observation of the acicular ferrite formation. Finally, the formed acicular ferrite amount is determined and inclusions are classified in active and inactive.

SCIENTIFIC APPROACH

The present study focuses on the specific modification of deoxidation and desulfurization products aiming in the creation of active nuclei for acicular ferrite. Two different steel compositions are analysed. Their compositions are listed in **Table 1**. The two steels only differ in the used deoxidizer: steel A is treated with titanium, steel B with silicon and calcium.

Table 1: Steel composition [wt.-%]

	C	**Mn**	**Si**	**Ca**	**Ti**	**S**	**O**	**N**
Steel A	0.230	1.500	-	-	0.050	0.008	0.005	0.002
Steel B	0.230	1.500	2.000	0.005	-	0.008	0.005	0.002

Both steels are investigated following a four-step method, which is illustrated in **Figure 1**.
The first step of the method is the thermodynamic calculation of the inclusion formation and modification. Therefor *FactSage 6.4* with the databases *FactPS*, *FToxid* and *FSstel* is used. So-called inclusion diagrams are created by the module *Phase Diagram*. Inclusion diagrams show the stable inclusion types at a defined temperature. In the present work the necessary amount of alloying elements to adjust a specific inclusion type is defined by the use of inclusion diagrams. By means of the module *Equilib* a process model was created, which simulates the stepwise process of Tammann furnace experiments. So-called solidification routes, also calculated by the module *Equilib*, depict the change of the inclusion landscape during solidification and the subsequent cooling.
Within the second step melting experiments in a Tammann type furnace (Ruhrstrat HRTK 32 Sond.) are performed, aiming in the production of steel samples with a defined and homogeneous distributed inclusion landscape. A detailed description of the Tammann type furnace can be found in [17]. All used raw materials are listed in **Table 2**. First, unalloyed steel is mixed with O-premelt to produce a melt with an initial content of 300 ppm oxygen and 80 ppm sulfur. Second, carbon granules and electrolytic manganese are added to reach a C-content of 0.230 % and a Mn-content of 1.500 %. By this the O-content of the melt is decreased to 0.014 %. After reaching the experimental temperature of 1600 °C (heating rate 10 °C/min) in the Tammann type furnace the samples are hold for 10 min at this temperature. During this time the melt is deoxidized with titanium reaching 0.050 % Ti, respectively silicon and calcium reaching 2.000 % Si and 0.005 % Ca. Special attention is paid to the stirring of the melt during the processing, to ensure a homogenous inclusion distribution. Finally, the sample is quenched rapidly to hinder inclusion flotation.

Table 2: Composition of raw materials [wt.-%]

	C	Mn	Si	Ca	Ti	S	O	Fe
unalloyed steel	0.004	0.066	-	-	-	0.006	-	99.924
O-premelt	0.001	0.075	-	-	-	0.009	0.175	99.740
C-granules	100	-	-	-	-	-	-	-
electrolytic Mn	-	100	-	-	-	-	-	-
FeTi	-	-	-	-	75	-	-	25
FeSiCa	-	-	56	16	-	-	-	28

Afterwards, within the third step, the produced samples are heat treated by a high temperature laser scanning confocal microscope (HT-LSCM). By HT-LSCM phase transitions can be observed in situ, which helps to gain essential information about the formation mechanism of acicular ferrite. The HT-LSCM consists of a laser scanning confocal microscope type VL2000DX, produced by Lasertec, an attached high temperature furnace type SVF17-SP and the associated hard- and software of Yonekura. A detailed description of the system as well as its function and advantages are to be found in [18–22]. The samples are first austenized at 1400 °C for 100 s and then cooled. Between 800 and 500 °C the cooling rate is 200 °C/min.

To quantify the inclusion's impact on the formation of acicular ferrite, the samples are metallographically analysed in the fourth step of the method. The prior austenite grain size can be determined by optical microscopy (OM). Because austenite grain boundaries are revealed by thermal etching in the course of the HT-LSCM treatment, no additional chemical etching is necessary. The analysis of the acicular ferrite amount in the microstructure is done after etching with nital, also using OM. OM is carried out with a Polyvar Pol microscope combined with a digital camera Clemex 3 megapixel. A detailed description of the OM investigations is given in [20, 23]. Additionally, the inclusion landscape is characterized by manual and automated analyses using the scanning electron microscopes (SEM) Fei Quanta 200 MK2 and Zeiss ULTRA 55, which are both equipped with an energy dispersive X-ray spectrometer (EDS) system of Oxford Instruments.

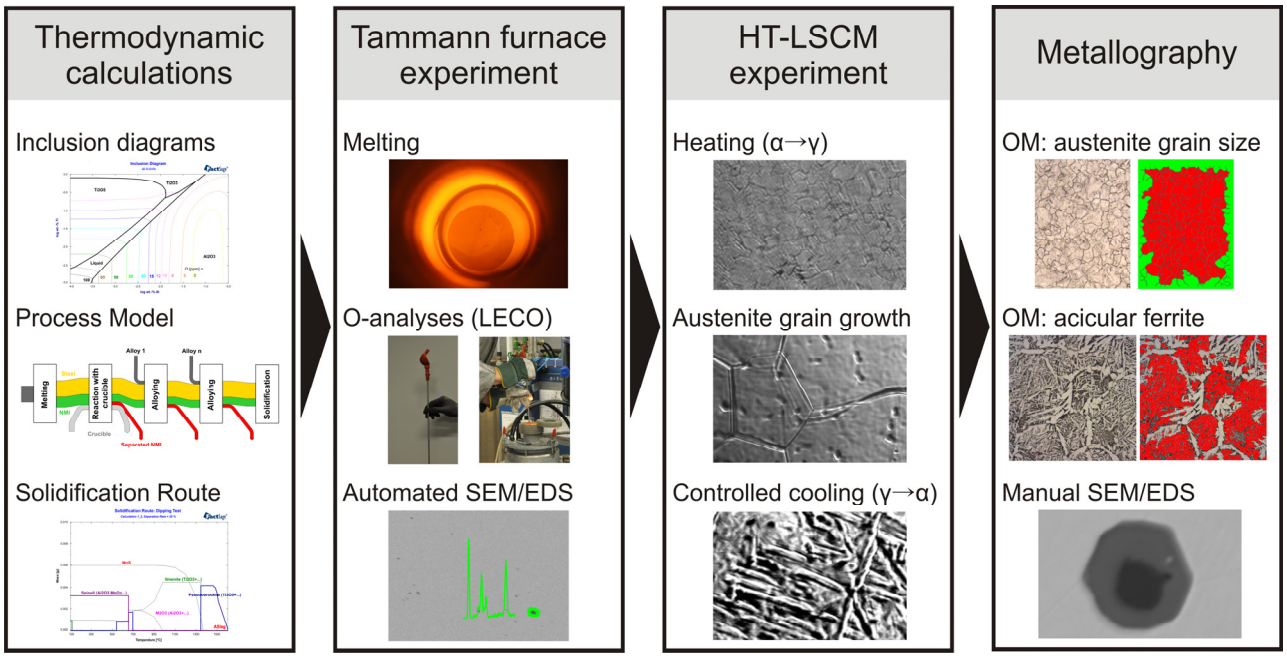

Figure 1: Experimental procedure for the investigation of non-metallic inclusions concerning their effect on the formation of acicular ferrite.

CREATION OF A DEFINED INCLUSION LANDSCAPE

To define the necessary steel composition for creating a particular inclusion landscape, inclusion diagrams are calculated by *FactSage 6.4*. Within inclusion diagrams two elements can be varied and the effect of this variation on the inclusion landscape at a defined temperature is illustrated. In **Figure 2** and **Figure 3** the influence of oxygen and sulfur on the type of NMI is shown. The shown inclusion diagrams are calculated for 1500 °C, because at the experimental temperature of 1600 °C no sulfidic phase is stable and therefore a prediction of sulfide inclusions would not be possible.

As it can be seen in **Figure 2,** in steel A only TiOx inclusions are stable at low O- and S-contents, which consist mainly of Ti-oxide and a small amount of Ti-Mn-oxide. If the S-content is increased MnS becomes stable. An increase in oxygen first leads to the formation of the phase ASlag, a liquid mixture of Mn-oxide, MnS, Fe-oxide, FeS and Ti-oxide. A further increase of the O-content stabilizes Mn-Ti-oxide and Monoxide (MnO with small contents of Fe-oxide and Ti-oxide). Within the present study an inclusion landscape consisting of TiOx, MnS and ASlag should be produced. These inclusion types are chosen, because they are described in literature to have a high potential to act as active nuclei for acicular ferrite. So, the target value for oxygen is set at 300 ppm and for sulfur at 80 ppm.

To compare different types of deoxidation products, next to the Ti-killed steel A, the Si-Ca-alloyed steel B is analysed. **Figure 3** shows the inclusion diagram for steel B, which illustrates that at low O- and S-contents Monoxide (CaO with small contents of Fe-oxide and Mn-oxide) and CaS are stable. If the S-content gets higher, also Ca-Si-oxide will form. An increase in oxygen results in the transformation of the Ca-Si-oxide phase to ASlag and further to ASlag+SiO_2. For steel B the phase ASlag consists of Mn-oxide, MnS, CaS, Fe-oxide, FeS, Si-oxide and Ca-oxide. To achieve comparable results for steel B the same O- and S-level as for steel A are set. According to the inclusion diagram this will form ASlag- and SiO_2-incusions.

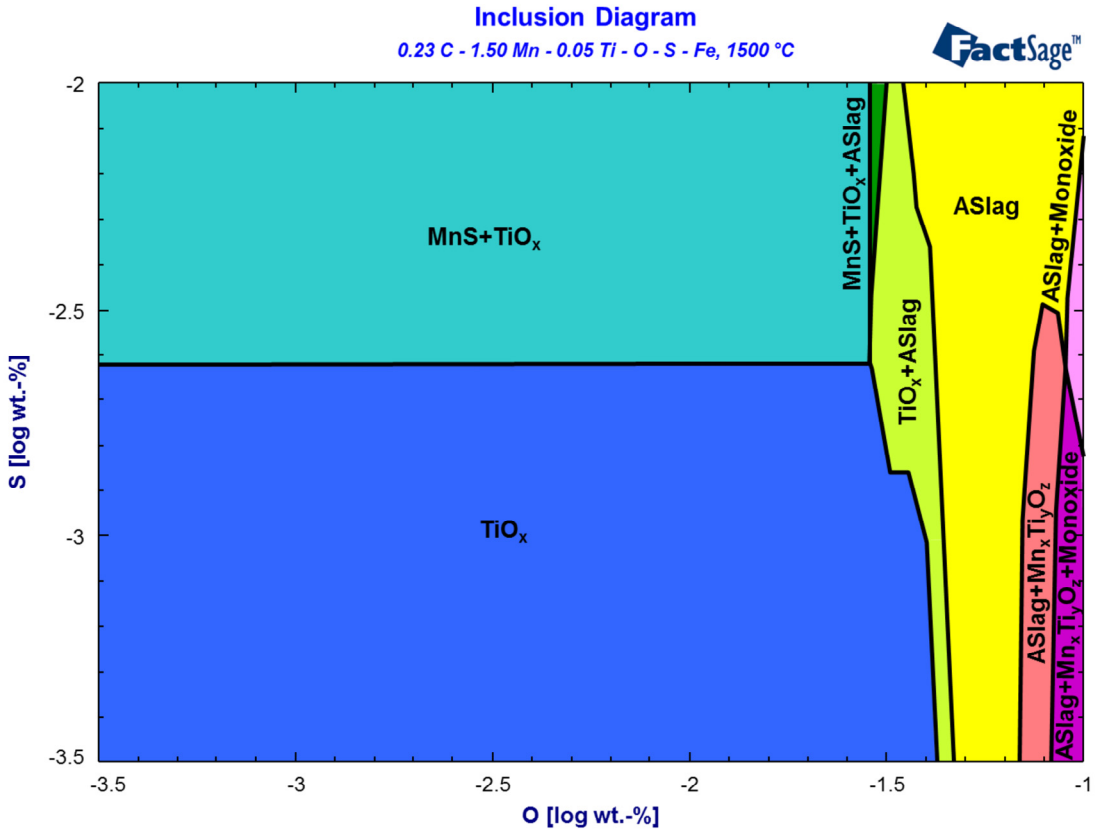

Figure 2: Inclusion diagram for steel A at a temperature of 1500°C.

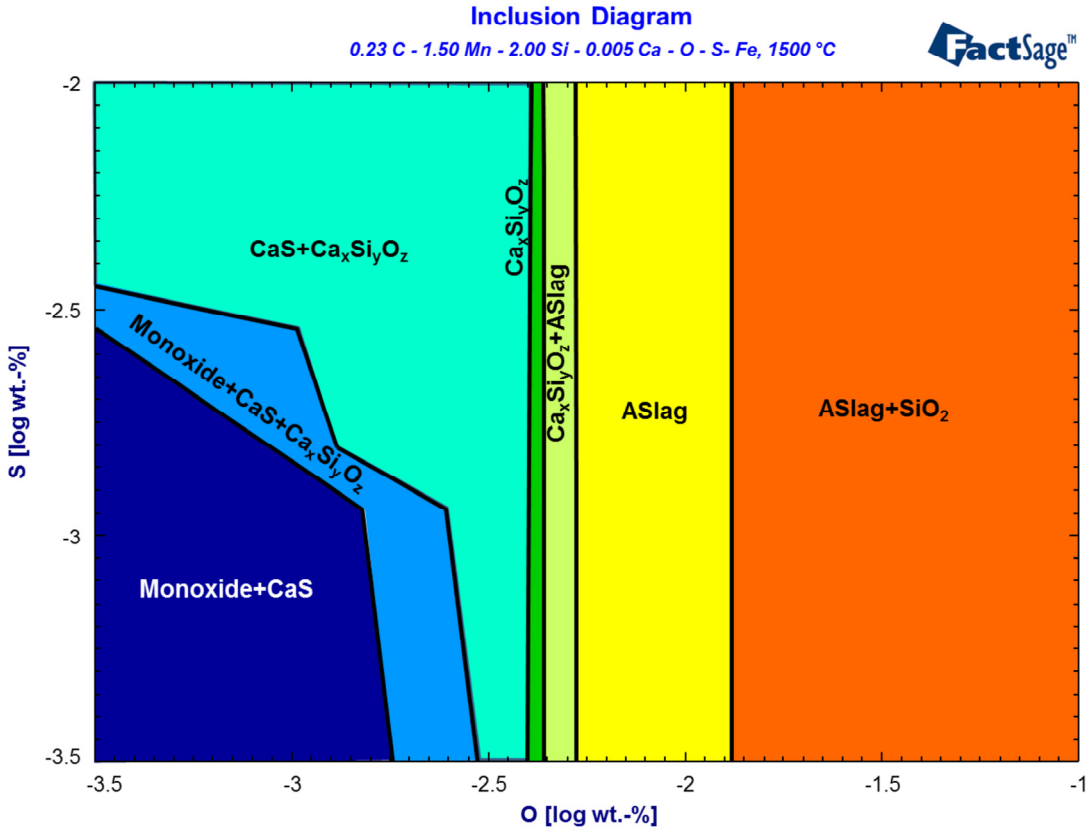

Figure 3: Inclusion diagram for steel B at a temperature of 1500°C.

Although inclusion diagrams are very useful for setting the melt composition, they do not really model a practical melting experiment in the Tammann type furnace. Neither the influence of the crucible material, the step-wise addition of the alloying elements, the flotation of NMI during the process nor the sample cooling to room temperature is considered. By the developed process model in *FactSage* the inclusion formation and modification during the practical experiment can be modeled, including:

- influence of the crucible
- inclusion landscape in raw material
- change of the inclusion landscape during cooling.

The process model for steel A is shown in **Figure 4** and is based on the steel composition determined by the inclusion diagram in **Figure 2**. Beside the chemical composition of the steel melt, also the $SiO_2 \cdot MnO$-, $SiO_2 \cdot MnO \cdot Al_2O_3$- and $MnO \cdot Al_2O_3$-inclusions already present in the used raw material are used as input for the first calculation step. After melting only ASlag inclusions are stable in the melt. In the next calculation step the reaction with the Al_2O_3 crucible is considered. The reaction of melt and crucible certainly happens throughout the experiment, but to simplify the model it is handled as a discrete reaction. However, the error due to this simplification may be small, because the products resulting from the *FactSage* calculation belong to infinite reaction time (equilibrium calculation). In the practical experiment the reaction happens continuously, but the equilibrium will not be reached due to the limited time. Through the contact of the melt with the Al_2O_3 crucible Al-spinel inclusions become stable and the amount of ASlag is reduced. Al-spinel consists mainly of $MnO \cdot Al_2O_3$, possibly with small amounts of $FeO \cdot Al_2O_3$. The remaining ASlag also contains Al_2O_3 after the contact with the crucible. A part of these inclusions separates before titanium is alloyed due to flotation or sticking at the crucible wall. The added titanium changes conditions of the stable inclusion types: half of the inclusions are then Corundum (Al_2O_3 with a low solubility for Ti-oxide) and half of them are ASlag. Before the melt solidifies, again inclusions are separated.

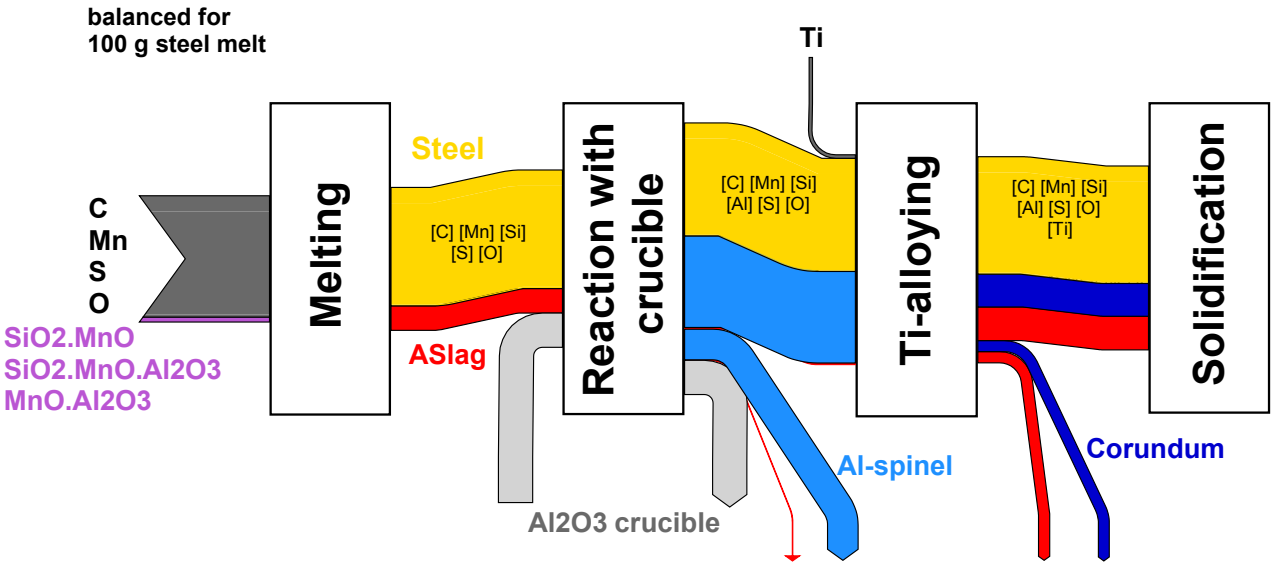

Figure 4: Thermodynamic model of melting steel A at 1600 °C in an alumina crucible.

To predict the final inclusion landscape at room temperature, the modification of NMI during cooling has to be considered by so-called solidification routes. But it should be pointed out that these solidification routes do not take kinetics into account, all results belong to the equilibrium stage. Hence, it is possible that the inclusion landscape determined analytically at room temperature differs from the calculated one. Some high-temperature phases, which shall dissolve during cooling according to *FactSage*, may still be found in the final sample due to the lack of time to reach equilibrium. The predicted inclusion landscape is compared to the measured one by automated SEM/EDS. The results of the SEM/EDS analyses for both steel grades are given in **Figure 5**.

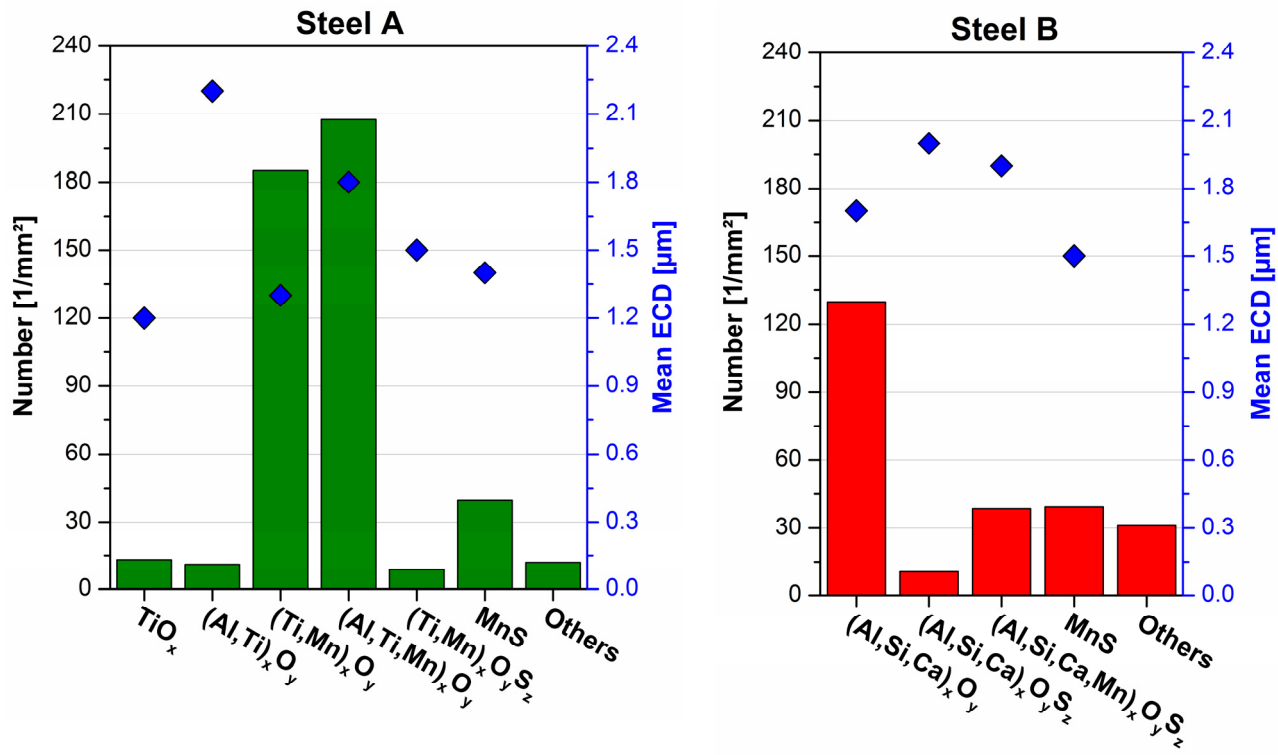

Figure 5: Detected NMI by automated SEM/EDS in steel A and B.

Figure 6 shows the solidification route for steel A. The calculation results are in good agreement with the SEM/EDS measurements of the final Tammann furnace sample:

- *FactSage* predicts oxides as the major inclusions type. The SEM/EDS results also show oxides as the largest part of inclusions in steel A. The oxides consist in both cases of Ti-oxide, Al-oxide and Mn-oxide.
- At 1600 °C only ASlag and Corundum particles are present. With decreasing temperature the ASlag phase becomes instable and should decompose to Corundum and TiOx. But due to the high cooling rate in the practical experiment ASlag-particles can still be found in the final sample.
- A further decrease in temperature leads to the precipitation of MnS. *FactSage* predicts the formation of MnS, which is also detected by SEM/EDS measurements.
- The formation of Al-spinel oxides below 700 °C is annunciated by *FactSage*, but this inclusion type was hardly found by SEM/EDS. A possible explanation for that is the low formation temperature, at which the driving force for chemical reactions is already low.

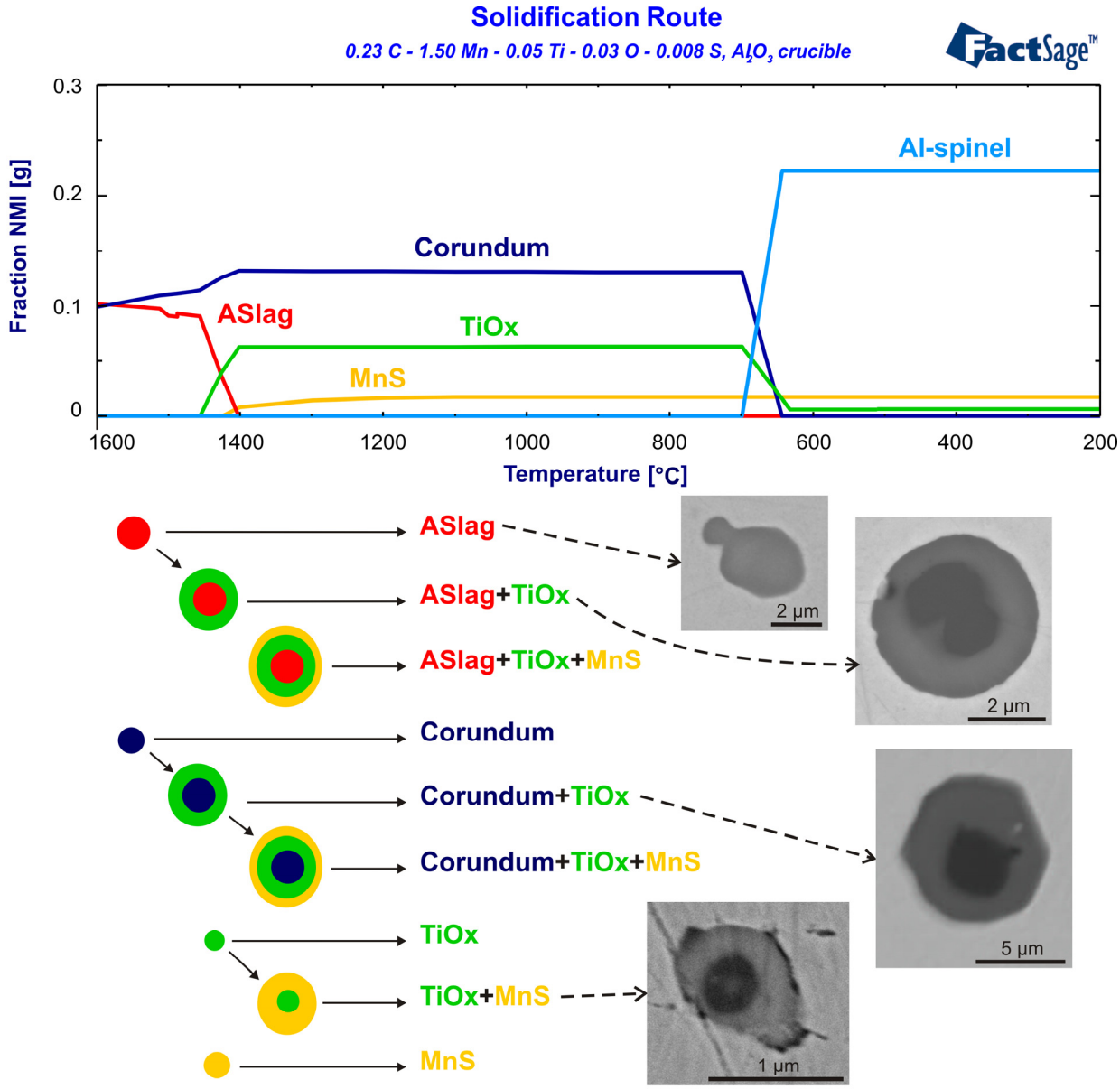

Figure 6: Solidification route for steel A.

In **Figure 7** the solidification route of steel B is presented. The comparison of these calculated results to the SEM/EDS output also shows a good accordance:

- Similar to steel A *FactSage* calculated oxides and MnS as the main inclusion types in steel B. Consistent with *FactSage* the majority of inclusions in the SEM/EDS measurement are oxidic, containing Al-, Ca- and Si-oxide, sometimes also Mn-oxide.
- At 1600 °C *FactSage* predicts ASlag and Corundum to be stable. With decreasing temperature ASlag decomposes to Corundum and Al-Si-Ca-oxide. As shown in **Figure 5** the main fraction of inclusions in steel B is analysed as Al-Si-Ca-oxide, either as pure oxide or as oxide with a sulfidic layer (oxisulfide).
- With decreasing temperature MnS becomes stable according to *FactSage* and also the SEM/EDS results show a significant amount of MnS.
- Like in steel A Al-spinel oxides should form below 700 °C, but again Al-spinel inclusions can hardly be detected by SEM/EDS.

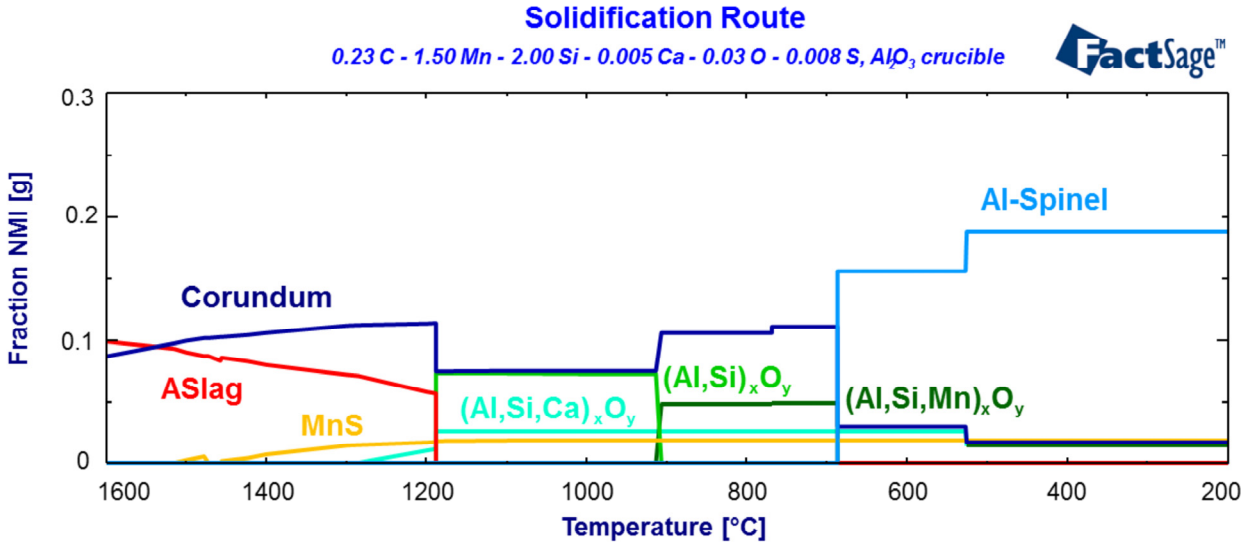

Figure 7: Solidification route for steel B.

Heterogeneous nucleation plays an essential role during cooling of the investigated steels. So, most of the inclusions detected by SEM/EDS are multiphase-inclusions. In steel A on the one hand MnS tends to nucleate on already present oxides, forming the favored inclusion type TiOx+MnS. One example of such an inclusion is shown in **Figure 8**. On the other hand also TiOx is often found as heterogeneous layer on other oxides like Corundum. Some examples of complex inclusions are illustrated in **Figure 6**. In steel B mainly sulfides are found to nucleate on oxides. But it should be mentioned, that SEM/EDS only displays the overall composition of an inclusion. Hence, it is not possible to identify e.g. a Corundum core inside Al-containing phases like Al-Si-Ca-oxide. Therefore it is conceivable, that the real amount of oxides nucleated heterogeneously is larger compared to the detected one.

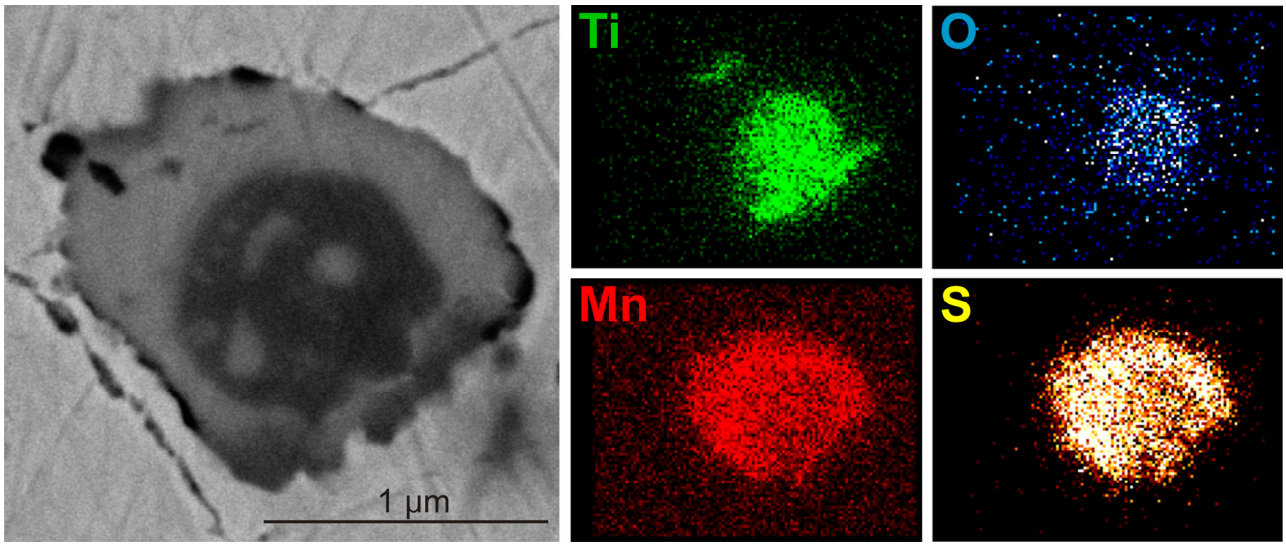

Figure 8: Ti-oxide inclusion with MnS-layer.

Aim of the thermodynamic calculations and the melting experiment was to produce steels with a defined inclusion landscape. Steel A should contain Ti-oxide or Ti-Mn-oxide inclusions with MnS-layer, which promote the formation of acicular ferrite microstructure according to literature [10, 14]. The Ti-oxide / Ti-Mn-oxides can be represented by TiOx or ASlag phase. Steel B was produced under comparable conditions, but instead of titanium Si and Ca were added for deoxidation. The primary determined inclusion types are Al-Si-Ca-oxides and MnS. For both steels the predicted inclusion landscapes by thermodynamics match very well with the inclusion landscapes analysed by SEM/EDS in the final samples.

EFFECT OF NON-METALLIC INCLUSIONS ON THE FORMATION OF ACICULAR FERRITE

The produced steels are heat treated by HT-LSCM to investigate the potential of the NMI to act as nuclei for acicular ferrite. The changes in the microstructure during the heat treatment of steel A are illustrated in **Figure 9**. After reaching the α→γ transition temperature austenite grains form and grow. During cooling the austenite grains transform to acicular ferrite (nucleating at non-metallic inclusions), Perlite, Widmannstätten ferrite (nucleating at grain boundaries) and grain boundary ferrite.

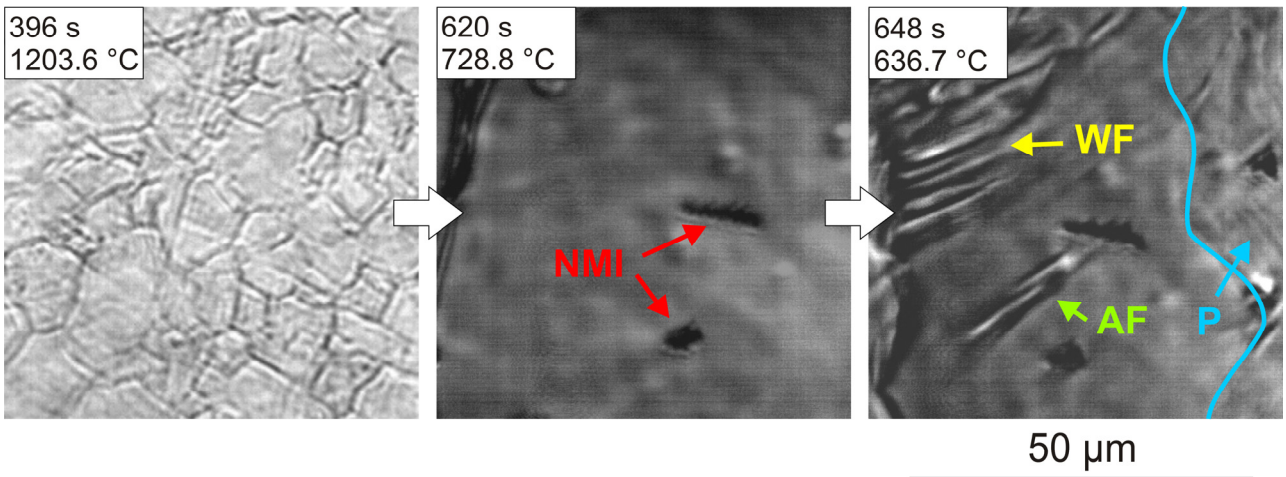

NMI … Non-metallic inclusions, AF … Acicular Ferrite
WF … Widmannstätten Ferrite, P … Perlite

Figure 9: Microstructure evolution in steel A during HT-LSCM treatment.

The heat treated samples are investigated concerning austenite grain size and acicular ferrite amount. A mean austenite grain size of about 130 µm in steel A and about 300 µm in steel B is determined. In **Figure 10** the microstructure of steel A and B after heat treatment by HT-LSCM is illustrated. The acicular ferrite amount in steel A is analysed as 60 %. Thus, steel A and the contained inclusions are active for acicular ferrite. In steel B significantly less acicular ferrite structures can be found, the microstructure mainly consists of bainite, perlite and grain boundary ferrite. Hence, for the tested cooling rate steel B is not active for acicular ferrite. But due to the huge impact of the cooling rate on the formation of acicular ferrite, further investigations with varying cooling rates will be necessary to identify the potency of the NMI in steel B to act as active nuclei.

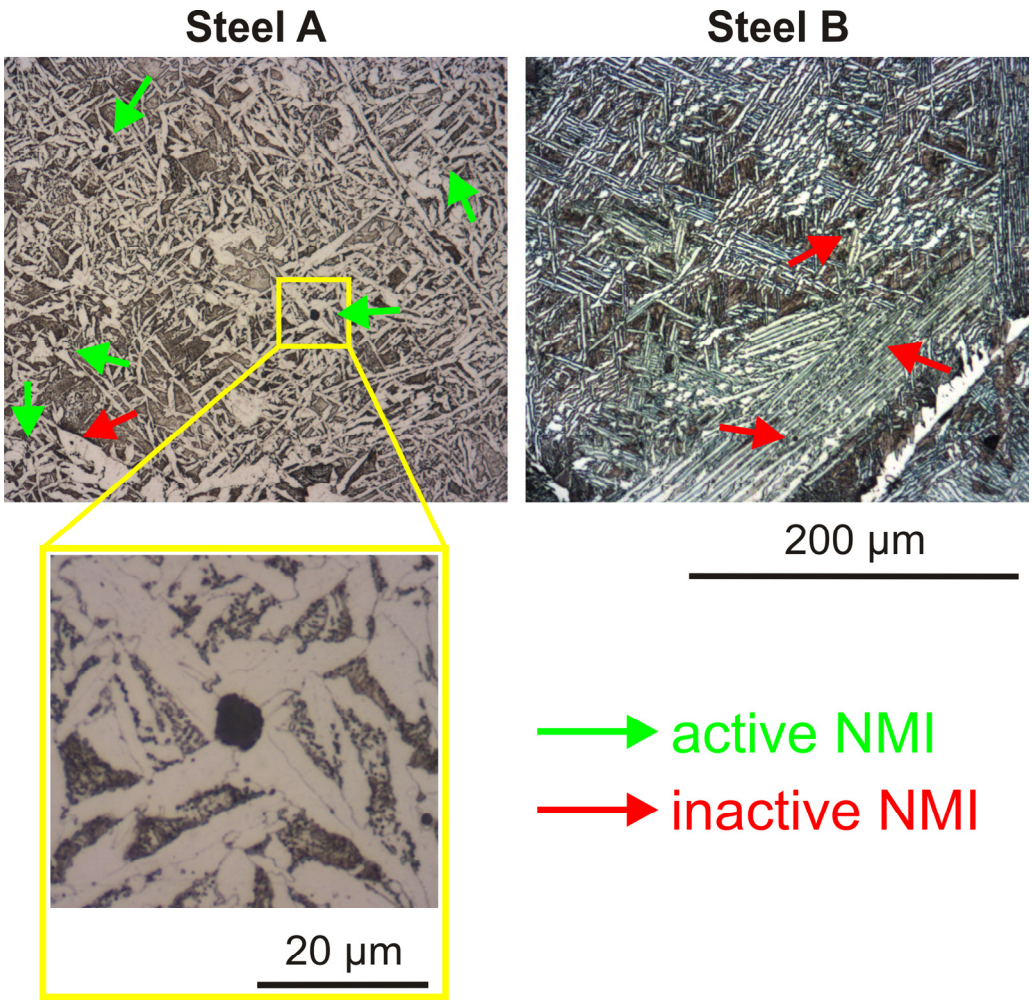

Figure 10: Microstructure after heat treatment by HT-LSCM.

SUMMARY & CONCLUSION

The focus of the present work was the evaluation of different endogenous inclusion types regarding their tendency for acicular ferrite formation in HSLA steels. Therefore only deoxidation and desulfurization products, which formed directly during steel making, were used. Two steels were investigated: steel A was deoxidized with titanium, steel B with silicon and calcium. The main conclusions can be summarized as follows:

- Thermodynamic calculations by *FactSage* including inclusion diagrams, process modelling and solidification routes are appropriate for the prediction of the inclusion formation and modification during metallurgical processing and for the design of melting experiments.

- Melting experiments were carried out on laboratory scale in a Tammann type furnace. The produced inclusion landscape was analysed by automated and manual SEM/EDS. The predicted inclusion landscape by *FactSage* is in very good agreement with the measurement results by SEM/EDS.
- Heat treatment by High Temperature Laser Scanning Confocal Microscopy (HT-LSCM) enables the in situ observation of the acicular ferrite formation and delivers therefore essential information about the formation mechanisms.
- Steel A mainly showed inclusions containing Ti, Mn, O and S, which are described as active in literature. By HT-LSCM the nucleation of acicular ferrite on this inclusion type was observable in situ.
- The majority of inclusions in Steel B consist of Al, Ca, Si, Mn, O and S. For the tested cooling rate this system did not show a high potential for acicular ferrite. Hence, further investigations will be done, to describe the tendency for acicular ferrite for varying cooling rates.

ACKNOWLEDGMENTS

The authors are grateful for the financial supports from the Federal Ministry for Transport, Innovation and Technology (bmvit) and the Austrian Science Fund (FWF): [TRP 266-N19]. Furthermore sincere thanks are expressed to the laboratories at voestalpine Stahl Donawitz GmbH for the assistance during sample analysis.

REFERENCES

[1] S. OGIBAYASHI: Advances in Technology of Oxide Metallurgy, Nippon Steel Technical Report 61 (1994), 70-76.

[2] H. GOTO, K.I. MIYAZAWA and T. KADOYA: Effect of the Composition of Oxide on the Reaction between Oxide and Sulfur during Solidification of Steels, ISIJ International 35 (1995), 1477–1482.

[3] H. GOTO, K.I. MIYAZAWA, W. YAMADA and K. TANAKA: Effect of Cooling Rate on Composition of Oxides Precipitated during Solidification of Steels, ISIJ International 35 (1995), 708–714.

[4] C. VAN DER EIJK, O. GRONG and J. HJELEN: Quantification of Inclusion-Stimulated Ferrite Nucleation in Wrought Steel using the SEM-EBSD Technique, Proceedings of the International Conference on Solid-Solid-Phase Transformations (1999), 1573–1576.

[5] D.J. ABSON, R.E. DOLBY and P.H.M. HART: The role of nonmetallic inclusions in ferrite nucleation in carbon steel weld metals, Proceedings of the International Conference on Trends in Steels and Consumables for Welding (1978), 75–101.

[6] R.C. COCHRANE and P.R. KIRKWOOD: The effect of oxygen on weld metal microstructure, Proceedings of the International Conference on Trends in Steels and Consumables for Welding (1978), 103–121.

[7] S. LIU and D.L. OLSON: The Influence of Inclusion Chemical Composition on Weld Metal Microstructure, Journal of Materials Engineering 9 (1987), 237–251.

[8] S.S. BABU, S.A. DAVID and J.M. VITEK: Effect of oxide inclusions on the solid state transformation on low-alloy steel fusion welds, Proceedings of the International Conference on Trends in Welding Research (1995), 1-7.

[9] S.S. BABU, F. REIDENBACH, S.A. DAVID, T. BÖLLINGHAUS and H. HOFFMEISTER: Effect of high energy density welding processes on inclusion and microstructure formation in steel welds, Science and Technology of Welding and Joining 4 (1999), 63–73.

[10] D.S. SARMA, A.V. KARASEV and P.G. JÖNSSON: On the Role of Non-metallic Inclusions in the Nucleation of Acicular Ferrite in Steels, ISIJ International 49(2009), 1063-1074.
[11] Z. ZHANG and R.A. FARRAR: Role of non-metallic inclusions in formation of acicular ferrite in low alloy weld metals, Materials Science and Technology 12 (1996), 237–260.
[12] J.M. GREGG and H.K.D.H. BHADESHIA: Solid-state nucleation of acicular ferrite on minerals added to molten steel, Acta Materialia 45 (1997), 739–748.
[13] M. ANDERSSON, J. JANIS, L. HALOPPA, M. KIVIÖ, P. NAVEAU, et al.: Grain size control in steel by means of dispersed non-metallic inclusions - GRAINCONT, Research Fund for Coal and Steel series - Final Report EUR 24991 (2011), 1-132.
[14] W. MU, P.G. JÖNSSON and K. NAKAJIMA: Effect of Sulfur Content on Inclusion and Microstructure Characteristics in Steels with Ti_2O_3 and TiO_2 Additions, ISIJ International 54 (2014), 2907–2916.
[15] S.C. PARK, I.H. JUNG, K.S. OH and H.G. LEE: Effect of Al on the Evolution of Non-metallic Inclusions in the Mn-Si-Ti-Mg Deoxidized Steel During Solidification: Experiments and Thermodynamic Calculations, ISIJ International 44 (2004), 1016-1023.
[16] I.H. JUNG, S.A. DECTEROV and A.D. PELTON: Computer Applications of Thermodynamic Databases to Inclusion Engineering, ISIJ International 44 (2004), 527–536.
[17] S.K. MICHELIC, M. HARTL and C. BERNHARD: Thermodynamic and Experimental Study on the Modification of Nonmetallic Inclusions Through the Contact with $CaO\text{-}Al_2O_3\text{-}MgO$ Slags, AISTech Proceedings –Volume II (2011), 617–626.
[18] C. BERNHARD, S. SCHIDER, A. SORMANN, G. XIA and S. ILIE: Erste Ergebnisse des neuen Hochtemperatur-Konfokalmikroskops am Lehrstuhl für Metallurgie, Berg- und Hüttenmännische Monatshefte 156 (2011), 161–167.
[19] P. PRESOLY, R. PIERER and C. BERNHARD: Identification of Defect Prone Peritectic Steel Grades by Analyzing High-Temperature Phase Transformations, Metallurgical and Materials Transactions 44A (2013), 5377-5388.
[20] P. PRESOLY, R. PIERER and C. BERNHARD: Linking up of HT-LSCM and DSC measurements to characterize phase diagrams of steels, IOP Conference Series - Materials Science and Engineering 33 (2012), 1-9.
[21] D. LODER., S.K. MICHELIC, A. MAYERHOFER., C. BERNHARD and R.J. DIPPENAAR: In situ observation of acicular ferrite formation using HT-LSCM: possibilities, challenges and influencing factors, Proceedings of MS&T (2014), 469–476.
[22] S. MICHELIC, J. GORIUPP, S. FEICHTINGER, Y.B. KANG, C. BERNHARD and J. SCHENK: Study on Oxide Inclusion Dissolution in Secondary Steelmaking Slags using High Temperature Confocal Scanning Laser Microscopy, Steel Research International 86 (2015), 1–11.
[23] D. LODER, S.K. MICHELIC and C. BERNHARD: Characterization of acicular ferrite microstructures using etching methods, optical microscopy and HT-LSCM, Sonderbände der praktischen Metallographie - Fortschritte in der Metallographie (2014), 125–130.